Generation of TOA Radiative Fluxes from the GERB Instrument Data. Part II: First Results.

N. Clerbaux[1], S. Dewitte, A. Ipe, C. Bertrand, L. Gonzalez, A. Joukoff

Royal Meteorological Institute of Belgium, Department of Observations, Section Remote Sensing from Space, Avenue Circulaire 3, B-1180 Brussels, Belgium.

Abstract

This second part of the paper presents the first results obtained with actual SEVIRI data in the RMIB GERB Processing (RGP) system. At this time, the calibration of the SEVIRI instrument seems sufficiently accurate and the different processings realized on this data seems to perform correctly. Nevertheless, a lot of validation activities remains to be done before the public release of the GERB data which is foreseen for mid–2004.

1 Introduction

The SEVIRI processing is an important part of the RMIB GERB Processing (RGP) system which has been implemented during the period 1998–2000. Since 1998, operational test of this processing is done using input data from Meteosat-5,6 and -7. The reception of SEVIRI data at the Royal Meteorological Institute of Belgium started the 29th of July 2003 and this paper describes the results obtained using this data in the processing. According to its use in the RGP, the instrument data seems to do not present problem. Also, the available calibration at this stage of the commisionning seems to be within the requirement and the accuracy of the spatial rectification seems sufficient. As shown hereafter, most of the RGP subsystems which use SEVIRI data as input appear to work correctly. Obviously, different validation activities remain to be done during the forecoming months.

2 SEVIRI Calibration

RMIB do not plan to perform calibration of the SEVIRI solar and thermal channels. The calibration coefficients provided by EUMETSAT in the HRIT files are used. For the solar channels (HRV, VIS0.6, VIS 0.8 and IR 1.6), the coefficients provided by Yves Govaerts (personal communication) are used. The calibration has been checked and will be monitored in the future. To validate the calibration, we have checked that the distribution of the observed narrow–band radiances for a particular slot (the 08/08/2003 at 12:00 UTC) is consistant with a data base of simulated SEVIRI NB radiances. Those simulated SEVIRI radiances are derived from a data base of spectral radiance curves generated at RMIB using the SBDART radiative transfer model for a large set of Earth–atmosphere conditions [*Clerbaux*, 2003c]. The figure (1) shows different scatter plots of pairs of NB radiances. Those graphs show that it does not appear significant problem with the calibration available some months after the launch. On the other hand, the

[1]Email: Nicolas.Clerbaux@oma.be

graphs illustrate some weaknesses in the data base of radiative transfer computations. (1) The presence of a too large percentage of snow covered surfaces with respect to what is actually observed by SEVIRI. (2) An overestimation of the radiance in the IR 8.7 band over hot desertic surfaces. This is due to the fact that the weak emissivity of the sand in this spectral band is not taken into account in the radiative transfer computations. And (3), also for desertic scenes, the simulated radiance in the IR 13.4 channel is overestimated with respect to the observed radiance. This indicates that there is not enough "dry atmospheric profiles" in our data base.

3 SEVIRI Spectral Modelling

The spectral modelling within the SEVIRI processing consists in the estimation of broadband radiances from the NB measurements. The quantities that have to be estimated are the filtered GERB SW and LW radiances as well as the unfiltered solar and thermal radiances. This is classicaly done using polynomial regressions on the NB radiances. The coefficients of the regressions are parameterized using the data base of radiative transfer computations introduced before.

The validation of this part of the processing is obvious because the estimated SW and LW radiances can be compared to the corresponding GERB measurements. The ratio between estimated and measured GERB filtered radiances are given in figure (2) for SW and LW. This comparison suffers from the currently poor accuracy of the geolocation of the GERB data. This is specially visible at the border of clouds and continents in the image of shortwave ratio. The images of GERB/SEVIRI ratio show that, in general, the SW spectral modelling performs well over the ocean, the vegetation and the clouds but fails over desert, where the estimated BB radiance is in excess of about 10% with respect to the measurements. At this time, this is explained as resulting of the surface spectral reflectance curves used in SBDART for sand surface. As for the SW, the LW spectral modelling performs correctly, except over the desert where an underestimation is here observed.

Validation and improvement of the SEVIRI NB–to–BB conversion will continue once improved geolocation for the GERB data will be available. This is expected to result in interesting SEVIRI NB–to–BB conversion formula's, possibly at the regional scale. Those improved regressions can be useful in the future for *GERB–like* data generation from SEVIRI alone, for instance in case of failure of the GERB instrument before the nominal life time of SEVIRI (7 years).

4 SEVIRI Scene identification

4.1 Introduction

The selection of the most–appropriated Angular Dependency Model (ADM) for the radiance–to–flux conversion needs a characterization of the field–of–view in terms of surface type, cloud fraction, cloud optical depth and cloud thermodynamical phase. The method that has implemented to retrieve those quantities and the first results obtained with SEVIRI are described hereafter.

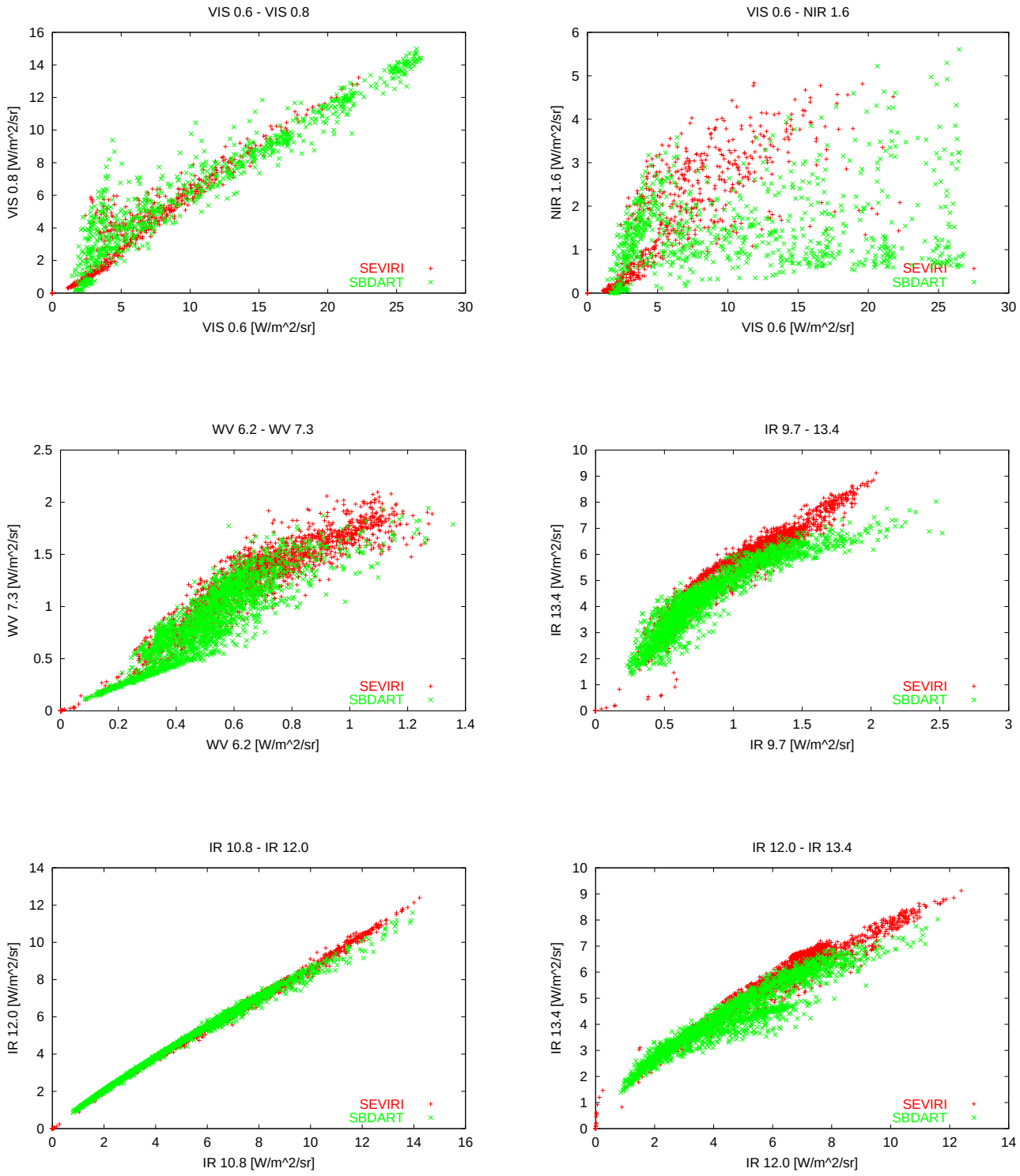

Figure 1: Various scatter plots of radiances in pairs of SEVIRI channels as observed by the instrument (+, in red) and as simulated by radiative transfer computation (x, in green).

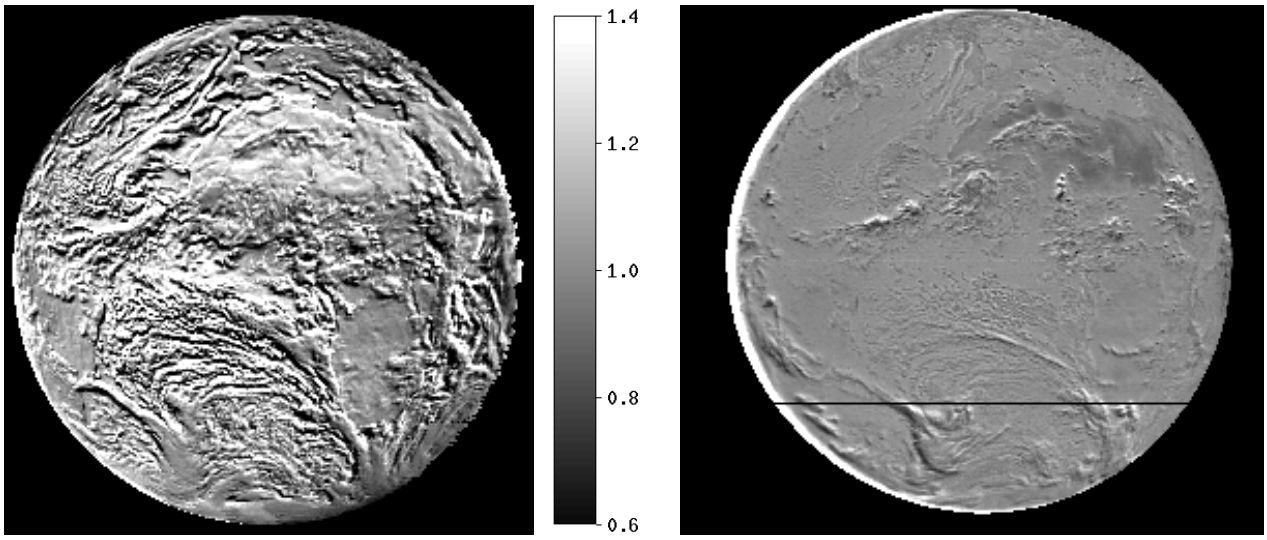

Figure 2: Ratio between the radiance measured by GERB and the corresponding radiance estimated from SEVIRI through the NB–to–BB conversion for 08/08/2003 - 12:00 UTC. Left is for shortwave and right is for longwave.

4.2 Surface characterization

The footprint is characterized as belonging to one of the following classes: ocean, moderate–to–high vegetation, low–to–moderate vegetation, dark desert, bright desert or snow. For this, a global IGBP classification [*Townshend*, 1994] at 1km resolution is used. The resulting map at the 3*3 SEVIRI pixel resolution is given in figure (3). Once available, fresh snow map derived over the MSG disk will be used (source to be defined). The spectral signature in the visible band images may also be used but the discrimination with ice cloud is known to be difficult. For clear ocean footprints, the angular modelling can be improved using information about surface wind speed and aerosol optical thickness as described in [*Loeb et al.*, 2003]. As for fresh snow, this information is not yet operationaly available over the MSG disk. In the meanwhile typical values (climatology) are used during the processing. Currently we are investigating the usefulness of ECMWF data in the processing.

4.3 Clear sky reflectance for VIS 0.6 and VIS 0.8 channels

The cloud identification takes advantage of the accurate estimation of the clear sky reflectance ρ_{cs} which is made possible by the geostationary orbit. The clear sky algorithm which has been implemented is described in [*Ipe et al.*, 2003] and figure (3) gives a color image built with the clear sky values in the VIS 0.6 and VIS 0.8 bands. The method has been validated for Meteosat–7 using human determination of cloud–free areas. The same visual approach will be done with SEVIRI. In this case, the task will be more easy, and probably more reliable, thanks to the use of false color visible band images of the VIS 0.6, VIS 0.8 and NIR 1.6 channels.

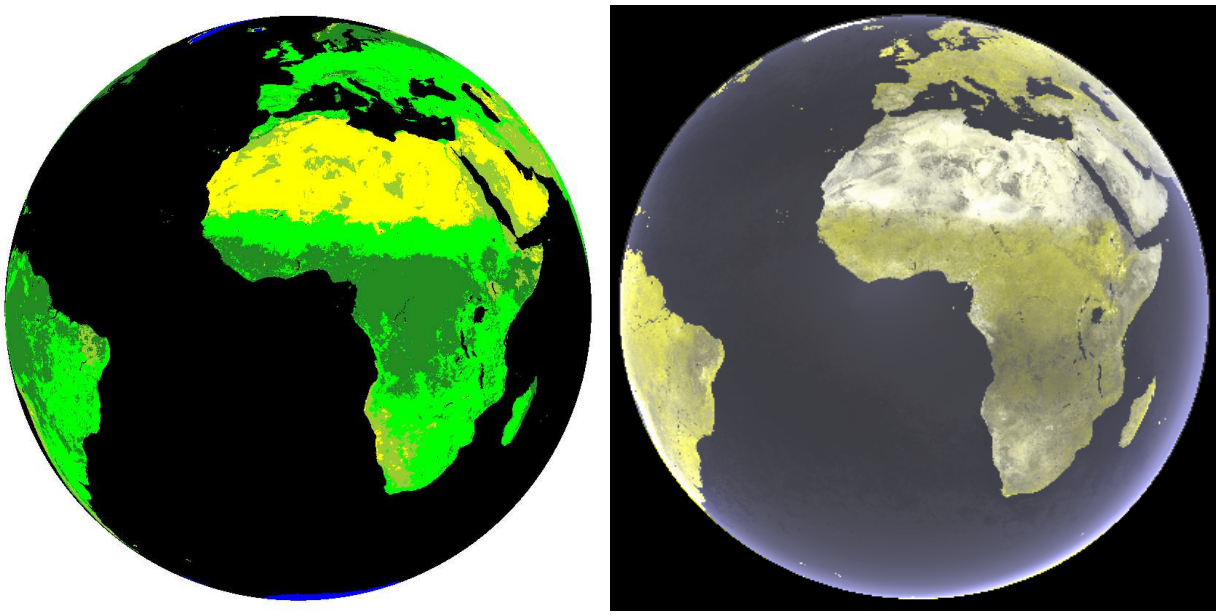

Figure 3: Left: Surface type. Right: False colour image of clear sky reflectance in the VIS 0.6 and the VIS 0.8 SEVIRI channels.

4.4 Cloud phase

The discrimination between water and ice thermodynamic phase for the cloud particles is important to apply the appropriate ADM but also to estimate correctly the cloud optical thickness through the use of different look–up–tables for water and ice clouds.

At this time, the cloud phase discrimination is only based on the brightness temperature in the IR 12.0 channel. For T_B below 245K the cloud is pure ice while for T_B higher than 265K the cloud is pure water. In between, the cloud is supposed to consist of a linear mix of the 2 phases. This simple method is known to fail in case of semi–transparent clouds (thin cirrus). In the future, the cloud phase discrimination will be improved by use of the NIR 1.6 channel. The figure (4, left) shows the scatter plot of the ratio of reflectance in the IR 1.6 and the VIS 0.6 with the brightness temperature in the IR 12.0 channel. For brightness temperature between 230K and 270K, the figure shows that the ratio of reflectances is informative to discriminate cloud phase.

4.5 Cloud optical thickness

In a first step, the algorithm decides, at the pixel scale, which visible band (VIS 0.6 or VIS 0.8) is the most–appropriated to estimate the cloud optical thickness. For this, the difference in NB reflectance between an optically thick cloud ($\tau = 128$) and the clear–sky is evaluated for the 2 bands:

$$\begin{aligned} \Delta_{0.6} &= \rho_{\text{cloud},0.6}(\theta_s, \theta_v, \phi) - \rho_{cs,0.6} \\ \Delta_{0.8} &= \rho_{\text{cloud},0.8}(\theta_s, \theta_v, \phi) - \rho_{cs,0.8} \end{aligned} \quad (1)$$

and the channel with the highest difference is selected. The figure (4, right) shows the result of this selection. The VIS 0.6 channel is selected over land surface while over the ocean the higher contrast is

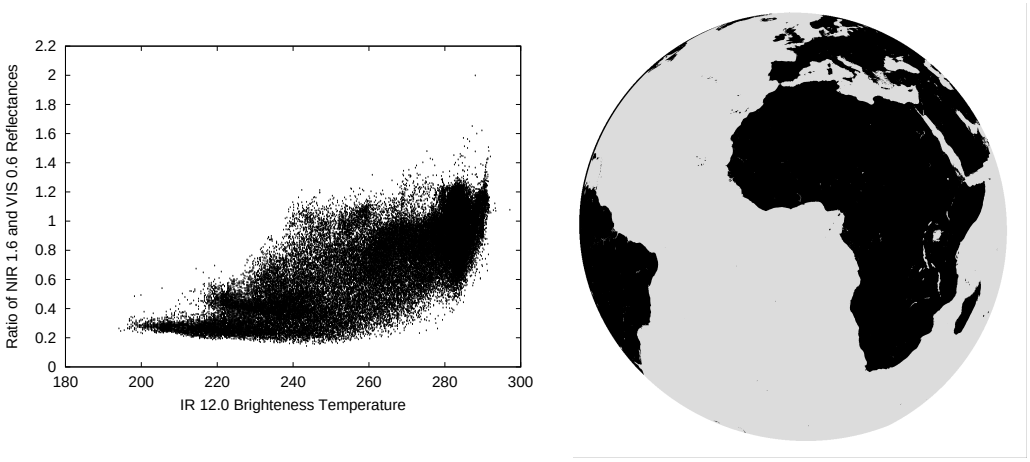

Figure 4: Left: Discrimination between ice and water clouds. Right: Image of the visible channel of SEVIRI presenting the more important contrast between clear–sky and overcast reflectance. black= VIS 0.6 , grey = VIS 0.8.

obtained in the VIS 0.8 band. This is in agreement with the result of previous studies: over the ocean the VIS 0.8 channel is more interesting because less sensitive to Raleygh scattering. Over land, the VIS 0.6 is selected bacause the channel is less sensitive to the vegetation than the VIS 0.8.

Once the most appropriated channel selected for a pixel, the cloud optical thickness τ is estimated using look–up–tables (LUT):

$$\tau = \tau(\rho, \rho_{cs}, \theta_v, \theta_s, \phi); \tag{2}$$

Those LUT were computed using STREAMER radiative transfer model for the 2 visible channels, for the 6 CERES surface types (ocean, dark and bright vegetation, dark and bright desert, snow) and for water and ice clouds phase. So, the estimation of the τ involves a total of 24 LUTs.

Once applied to Meteosat, we have checked that the cloud identification in term of cloud phase and cloud optical depth is consistant with the VIRS cloud characterisation performed by the CERES team. The same validation will be done with SEVIRI.

4.6 Cloud fraction

In a second step, a cloud mask is built by thresholding the cloud optical depth. The cloud fraction is then derived for 3x3 pixel boxes (i.e. 10 km resolution) and for the GERB footprints. Finally, the averaged cloud optical depth and thermodynamic phase is recomputed over the cloudy part of the boxes.

5 Angular Modeling

At this step, the fluxes are estimated from the unfiltered radiances. This requires the use of a model, R, accounting for the angular distribution of the radiance field at the TOA:

$$F_{LW} = \frac{\pi L_{LW}}{R(\theta_v)}$$

$$F_{SW} = \frac{\pi L_{SW}}{R(\theta_s, \theta_v, \phi)} \quad (3)$$

where θ_s and θ_v are the solar and viewing zenith angles and ϕ is the relative azimuth angle.

For the short wave radiation, the state–of–the–art models are the set of 592 models $R(\theta_s, \theta_v, \phi_r)$ derived by the CERES inversion team from 8 months of data from the CERES instrument on the Tropical Rainfall Measuring Mission (TRMM) satellite as described in [*Loeb et al.*, 2003]. Each model is representative for a given range of surface and cloud cover conditions. A set of ADMs is only valid for a given footprint size. For CERES–TRMM the footprint size at the subsatellite point is 10x10 km which prohibits their direct use for the GERB footprint. For this reason, the ADMs are applied on the SEVIRI estimate of the broadband unfiltered radiances (L_{SW} and L_{LW} in the Eq. 3) over boxes of 3x3 SEVIRI pixels. As the above cloud identification relies on the SEVIRI visible channels, it can not be used during night time. This is not a problem because in this case there is no need for ADM selection as there is no solar reflected radiation in Eq. (3).

For the long wave, the CERES–TRMM ADMs are not used because night time cloud identification is outside the scope of the GERB project. We plan to use cloud identification from the EUMETSAT Nowcasting Satellite Application Facility, once available. In the meanwhile, a modelling of the limb darkening based on the thermal measurements of SEVIRI has been implemented as described in [*Clerbaux et al.*, 2002(a)]

$$R(\theta_v) = R(\theta_v, L_{6.2\mu m}, L_{7.3\mu m}, L_{8.7\mu m}, L_{9.7\mu m}, L_{10.8\mu m}, L_{12\mu m}, L_{13.4\mu m}) \quad (4)$$

This approach is similar to the implementation of Schmetz and Liu (1988) for Meteosat. As the parameterization of Eq. (4) has been done using plane-parallel radiative transfer computations, the approach leads to an underestimation of the anisotropy over broken cloud fields. As the CERES–TRMM models, this model does not depend on the azimuthal angle of observation. Nevertheless, it has been shown that the azimuthal anisotropy over dry and mountainous regions may lead to a significant overestimation of the flux from the geostationary orbit [*Clerbaux et al.*, 2003(b)]. Indeed, GERB is always observing the southern faces of the mountains in the northern hemisphere and the northern faces in the southern hemisphere. Currently, those limitations are not compensated for.

A simple validation of the angular modelling for the thermal radiation consists to estimate the OLR for simultaneous Meteosat-7 (located at 0° longitude) and from Meteosat-5 (located at 63°E) data in the overlapping region. Those OLR are then averaged over 6 boxes having 10.5° extension in longitude ([0°:10.5°],[10.5°:21°], ..., [52.5°:63°]) and from 20S to 20N degrees latitude. This validation method indicates that the limb–darkening is not totally corrected with our model, at least in the tropical region.

6 Conclusions

According to its role within the RGP, the use of the first SEVIRI data didn't indicate any problem. The data looks like we were expecting the data to be. The calibration seems to be within the requirement and the accuracy of the rectification seems sufficient. Most of the SEVIRI based subsystems are working correctly even if some validations remain to be done during the forecoming months. A pre–operational system is expected to be operational for the end of october 2003. This system will allow to run the entire GERB/SEVIRI processing system in near–real time.

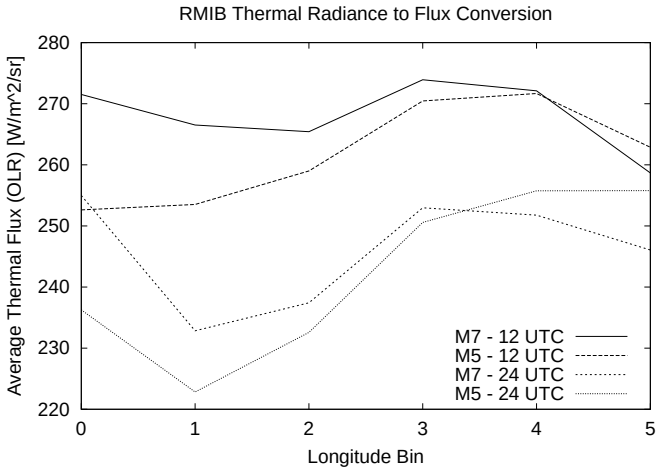

Figure 5: Mean OLR estimated in longitude boxes over the Equator from Meteosat-7 and from Meteosat-5. If the angular modelling is perfect, we expect the curves to be parallel.

References

[1] Clerbaux, N. and Dewitte, S. and Gonzalez, L. and Bertand, C. and Nicula, B. and Ipe, A., (2003,a) Outgoing Longwave Flux Estimation: Improvement of Angular Modelling Using Spectral Information, *Remote. Sens. Environ.*, 85, pp 389–395.

[2] Clerbaux, N. and Ipe, A. and Bertrand, C. and Dewitte S. and Nicula, B. and Gonzalez, L., (2003,b) Evidence of Azimuthal Anisotropy for the Thermal Infrared Radiation Leaving the Earth's Atmosphere, *Int. Journal of Remote. Sens.*, 24, pp 3005–3010.

[3] Clerbaux, N. (2003,c) Generation of a Data Base of Spectral Radiance Curves. *Technical Note MSG-RMIB-GE-TN-0030*, available on http://gerb.oma.be.

[4] Ipe, A. and Clerbaux, N. and Bertrand, C. and Dewitte S. and Gonzalez, L, (2003) Pixel–Scale Composite TOA Clear–Sky Reflectances for Meteosat–7 Visible Data, *Journal of Geophysical Research*, in press.

[5] Loeb, N.G. and Smith, N.M. and Kato, S. and Miller, W.F. and Gupta, S.K. and Minnis, P. and Wielicki,B.A. (2003) Angular distribution models for top-of-atmosphere radiative flux estimation from the Clouds and the Earth's Radiant Energy System instrument on the Tropical Rainfall Measuring Mission Satellite. Part I: Methodology *J. Appl. Meteor.*, 42, 240–265.

[6] Schmetz, J. and Liu, Q., (1988) Outgoing longwave radiation and its diurnal variation at regional scales derived from METEOSAT, *Journal of Geophysical Research*, 93, pp 11192–11204.

[7] Townshend, J.R.G. and Justice, C.O. and Skole, D. and Malingreau, J.-P. and Cihlar, J. and Teillet, P.M. and Sadowski, F. and and Ruttenberg, S., (1994) The 1-km AVHRR global data set: needs of the International Geosphere Biosphere Program, *Int. Jour. Rem. Sens., 15, 3319–3332.*